Geophysica (1983), Vol. 20, No. 1, pp. 5–25
Printed in Finland

551.583.13

ON DETERMINATIONS OF LIMIT CYCLES

by

A. WIIN-NIELSEN

World Meteorological Organization
Geneva, Switzerland

Abstract

The paper describes a comparative study of two methods of determining a limit cycle in low-order systems. One method is simply a numerical determination of the limit cycle by finite difference integrations in time. The second method depends on one or several transformations of the basic equations into polar co-ordinates. It is known that the second approximate method for certain equations is accurate close to a Hopf bifurcation point. The comparisons show that for the systems investigated here the region of good accuracy is limited to a relatively narrow region in parameter space close to the curve indicating bifurcation.

The two examples used for the comparative study are a sub-system of the climate system describing the interaction between the ocean temperature and the extent of the sea ice, and a predator-prey system of two competing populations.

1. *Introduction*

In many investigations of various low-order systems it is of interest to explore the stability properties of the system and to determine whether or not limit cycles exist. While the stability characteristics normally can be analysed using the standard methods of small perturbations it is much more difficult to determine the existence of the limit cycles, and they must normally be determined by numerical integrations of the equations. These time integrations are forward in time for unstable steady states and backward in time for stable states.

The problem of limit cycles is of interest in a number of low-order systems which illustrate the behaviour of simple climate models or sub-systems of more

comprehensive climate models such as those investigated by KÄLLEN *et al.* (1979), SALTZMAN *et al.* (1981), SALTZMAN and MORITZ (1980), SALTZMAN (1982) and KÄLLEN and WIIN-NIELSEN (1980).

This note contains a brief description of limit cycles in their most simple form (Section 2). The following sections give some examples in which the limit cycles are determined numerically and compared with an approximate method of determining them. It turns out that the approximate method is useful only in cases where the amplification rate is small.

2. *Limit cycles*

Let us start by considering a potential function $F(r)$. An example is shown in Figure 1. As long as $F(r)$ is a function of r only, the equation of motion is

$$\frac{dr}{dt} = -\frac{df}{dr} \tag{2.1}$$

It is seen by inspection of Figure 1 that there are three steady states at $r = 0$, 1 and 2. Furthermore $r = 0$ and $r = 2$ are stable, while $r = 1$ is unstable. The maximum between $r = 0$ and $r = 2$ is referred to as the potential barrier.

I magine now that the curve $f(r)$ is rotated around the vertical axis with angular velocity ω. We obtain then a rotation surface, and the equations for motion on

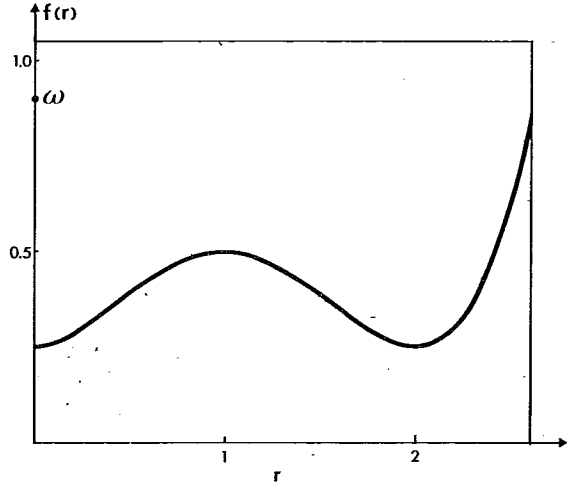

Figure 1. Example of a rotational, potential surface with an unstable and a stable limit cycle.

this surface are, in polar co-ordinates:

$$\begin{aligned} \frac{dr}{dt} &= -\frac{df}{dr} \\ \frac{d\phi}{dt} &= \omega \end{aligned} \tag{2.2}$$

A particle moving on the surface will either fall into the centre (0, 0) which is the only steady state of the system or move to $r = 2$, and it will then continue to move in the minimum of the rotation surface. It is for this reason that the circle $r = 2$, $\dot{\phi} = \omega$ is called a limit cycle.

The same situation can equally well be expressed in ordinary co-ordinates (x, y). In this case we have

$$x = r\cos\phi, \quad y = r\sin\phi \tag{2.3}$$

and

$$\begin{aligned} \frac{dx}{dt} &= \cos\phi\,\frac{dr}{dt} - r\sin\phi\,\frac{d\phi}{dt} \\ \frac{dy}{dt} &= \sin\phi\,\frac{dr}{dt} + r\cos\phi\,\frac{d\phi}{dt} \end{aligned} \tag{2.4}$$

Using (2.3) and (2.4) we may transform the system (2.2) into the following system:

$$\begin{aligned} \frac{dx}{dt} &= -\cos\phi\,\frac{df}{dr} - \omega y \\ \frac{dy}{dt} &= -\sin\phi\,\frac{df}{dr} + \omega x \end{aligned} \tag{2.5}$$

For the rotation surface we have

$$\frac{\partial f}{\partial x} = \frac{\partial r}{\partial x}\frac{df}{dr} = \frac{x}{(x^2+y^2)^{1/2}}\frac{df}{dr} = \cos\phi\,\frac{df}{dr} \tag{2.6}$$

and a similar expression for $\partial f/\partial y$. We may therefore write (2.5) in the form

$$\begin{aligned} \frac{dx}{dt} &= -\frac{\partial f}{\partial x} - \omega y \\ \frac{dy}{dt} &= -\frac{\partial f}{\partial y} + \omega x \end{aligned} \tag{2.7}$$

The equations (2.2) or (2.7) are special because it has been assumed from the beginning that one of the driving forces is a potential. This is not normally the case in the low order systems appearing in the literature, but the example is chosen here because it gives a visual determination of the limit cycle and because the technique used here is also applied later in determining the limit cycles by approximation.

Before leaving these preliminary remarks we give a specific example. Assume that

$$f(r) = f_0 - \tfrac{1}{4}\beta r^2(2-r^2)$$

from which it follows that

$$f'(r) = -\beta r(1-r^2), \quad f''(r) = -\beta(1-3r^2)$$

$f(r)$ is shown in Figure 2 for $f_0 = 1$, $\beta = 1$.

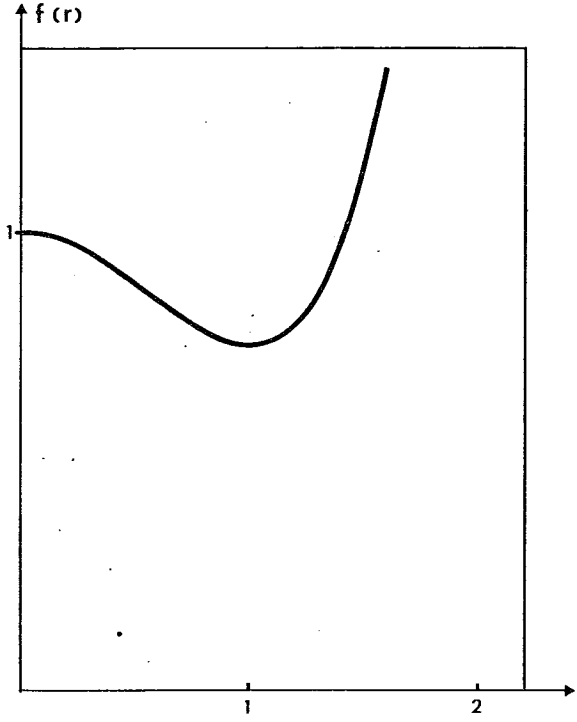

Figure 2. Example of a rotational, potential surface with a stable limit cycle.

For this example we have

$$f(x,y) = f_0 - \tfrac{1}{4}\beta(x^2+y^2)(2-x^2-y^2)$$

and it therefore follows that the equations corresponding to (2.7) are:

$$\frac{dx}{dt} = \beta x - \omega y - \beta(x^2+y^2)x$$

$$\frac{dy}{dt} = \omega x + \beta y - \beta(x^2+y^2)y$$

It is obvious from Figure 2 and the expressions for $f(r)$, $f'(r)$ and $f''(r)$ that $(0,0)$ is an unstable steady state and that a stable limit cycle is $x^2+y^2=1$. These results can also be obtained from the above equations. If $x^2+y^2=1$ we see that the equations reduce to

$$\frac{dx}{dt} = -\omega y$$

$$\frac{dy}{dt} = \omega x$$

which represent a rotation with angular velocity ω.

3. *A subsystem of the climate*

We shall begin by discussing a subsystem of the total climate system proposed by SALTZMAN *et al.* (1981). This simple system deals with the interaction between the ocean temperature and the extent of the ice in the ocean. The behaviour of this system has been investigated in detail by the authors quoted above, and they have found, among other properties, that the system has a stable limit cycle for realistic parameter values. In this section we shall compare numerically determined limit cycles with those obtained from an approximation method described below.

The two variables in the system are the deviation of the sine of the latitude of the sea ice extent from the steady state and the excess mean ocean surface temperature. The original equations are rescaled into non-dimensional equations, and after rescaling they appear in the following form:

$$\frac{d\eta}{dt} = -\eta + \theta$$

$$\frac{d\theta}{dt} = -a\eta + b\theta - \eta^2\theta \qquad (3.1)$$

Using the standard values quoted by the authors we have $a = 6.4$ and $b = 4$. The system (3.1) has always the steady state $(\eta, \theta) = (0,0)$. No additional steady states are possible for $b < a$. The eigenvalues of (3.1) are

$$\sigma = \frac{b-1}{2} \pm \mathrm{i} \sqrt{(a-b) - \left(\frac{b-1}{2}\right)^2} \tag{3.2}$$

and thus, stable limit cycles may exist if $b > 1$ and the radicand is positive. The latter condition leads to

$$b \leqslant 2\sqrt{a} - 1 \tag{3.3}$$

Using $a = 6.4$ we find that $b \leqslant 4.06$. It is thus seen that the recommended values of $a = 6.4$ and $b = 4$ satisfies the condition, but a slightly larger value of b would lead to σ becoming real and thus imply exponential growth or decay of a non-oscillatory nature. Figure 3 shows the stability properties as a function of a and b. The unstable oscillatory region of interest is marked U, 0. Limiting ourselves to this region we may write (3.2) in the form

$$\sigma = \beta \pm i\omega, \quad \beta > 0, \ \omega > 0 \tag{3.4}$$

A comparison between (3.4) and (3.2) shows that

$$\begin{aligned} b &= 1 + 2\beta \\ a &= (1+\beta)^2 + \omega^2 \end{aligned} \tag{3.5}$$

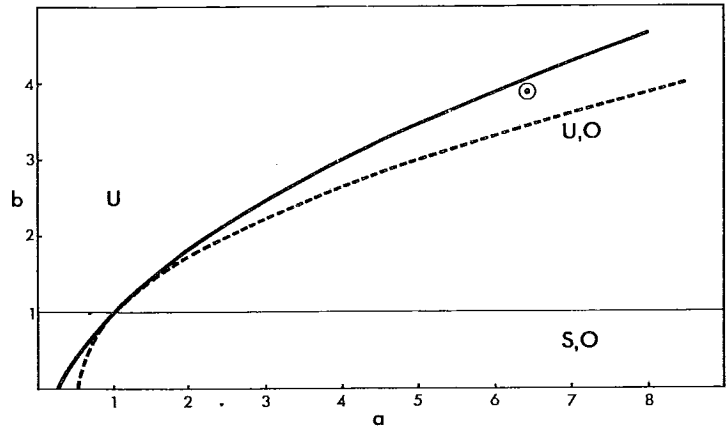

Figure 3. Stability diagram. Full curve represents the limit below which unstable, oscillatory motion will occur as long as $b > 1$ (horizontal line). The dashed line is $\beta = \omega$.

Although the present system does not possess a potential function it may nevertheless be an advantage to transform it into polar co-ordinates because these equations may indicate suitable approximations. The transformations are carried out in two steps. We define first a transformation as follows:

$$\begin{Bmatrix} \eta \\ \theta \end{Bmatrix} = \begin{Bmatrix} 1 & 1 \\ 1+\beta+i\omega & 1+\beta-i\omega \end{Bmatrix} \begin{Bmatrix} Z \\ Z_\star \end{Bmatrix} \tag{3.6}$$

transforming (η, θ) into a complex plane where Z and $Z_\star$ are complex conjugate numbers. The column vectors in the transformation matrix are the eigenvectors for the system (3.1) considering only the linear terms. The second step is simply to express Z and $Z_\star$ in the form of polar co-ordinates

$$\begin{aligned} Z &= re^{i\phi} = r\cos\phi + ir\sin\phi = r_c + ir_s \\ Z_\star &= re^{-i\phi} = r\cos\phi - ir\sin\phi = r_c - ir_s \end{aligned} \tag{3.7}$$

Using (3.6) and (3.7) it is easy to see that

$$\begin{aligned} \eta &= 2r_c \\ \theta &= 2(1+\beta)r_c - 2\omega r_s \end{aligned} \tag{3.8}$$

Inserting (3.8) in (3.1) we derive the equations

$$\begin{aligned} \frac{dr_c}{dt} &= \beta r_c - \omega r_s \\ \frac{dr_s}{dt} &= \beta r_s + \omega r_c + 4\frac{(1+\beta)}{\omega} r_c^3 - 4r_c^2 r_s \end{aligned} \tag{3.9}$$

The final step is to develop equations for dr/dt and $d\phi/dt$. These are obtained by noticing that

$$\begin{aligned} \frac{dr_c}{dt} &= \cos\phi \frac{dr}{dt} - r\sin\phi \frac{d\phi}{dt} \\ \frac{dr_s}{dt} &= \sin\phi \frac{dr}{dt} + r\cos\phi \frac{d\phi}{dt} \end{aligned} \tag{3.10}$$

Combining (3.10) and (3.9) we obtain

$$\begin{aligned}\frac{dr}{dt} &= \beta r + 4\frac{(1+\beta)}{\omega} r^3\cos^3\phi\sin\phi - 4r^3\cos^2\phi\sin^2\phi \\ r\frac{d\phi}{dt} &= \omega r + r\frac{(1+\beta)}{\omega} r^3\cos^4\phi - 4r^3\cos^3\phi\sin\phi\end{aligned} \tag{3.11}$$

The final equations are derived by expressing the trigonometric combinations in (3.11) in terms of $\cos(n\phi)$ and $\sin(n\phi)$. The purpose of this operation is to isolate those terms which vary slowly or rapidly in terms of ϕ. We note that

$$\begin{aligned}\cos^3\phi\sin\phi &= \tfrac{1}{4}\sin(2\phi) + \tfrac{1}{8}\sin(4\phi) \\ \cos^2\phi\sin^2\phi &= \tfrac{1}{8} - \tfrac{1}{8}\cos(4\phi) \\ \cos^4\phi &= \tfrac{3}{8} + \tfrac{1}{2}\cos(2\phi) + \tfrac{1}{8}\cos(4\phi)\end{aligned} \tag{3.12}$$

The final equations are:

$$\begin{aligned}\frac{dr}{dt} &= \beta r - \tfrac{1}{2}r^3 + \frac{1+\beta}{\omega} r^3\sin(2\phi) + \tfrac{1}{2}r^3\cos(4\phi) + \tfrac{1}{2}\frac{(1+\beta)}{\omega} r^3\sin(4\phi) \\ \frac{d\phi}{dt} &= \omega + \tfrac{3}{2}\frac{(1+\beta)}{\omega} r^2 + \frac{2(1+\beta)}{\omega} r^2\cos(2\phi) - r^2\sin(2\phi) + \tfrac{1}{2}\frac{(1+\beta)}{\omega} r^2\cos(4\phi) \\ &\quad - \tfrac{1}{2}r^2\sin(4\phi)\end{aligned} \tag{3.13}$$

The system (3.13) is equivalent to (3.1) as long as the eigenvalues have the form (3.4). No additional approximations have been made in the formal derivations. At the same time (3.13) looks more complicated than (3.1). The advantage of (3.13) should be that the first two terms in each of the equations are independent of ϕ while the remaining terms oscillate due to the dependence on ϕ. The argument normally made at this stage is that the oscillating terms may have little influence on the solution at large values of t and therefore on the stable limit cycle. It is furthermore stated that this argument in a strict sense holds only when $\beta/\omega \ll 1$. It is difficult to understand why these arguments should be true in all cases because (3.13) contains in each equation terms which are comparable to the first terms whenever they attain their maximum and minimum values. The curve $\beta = \omega$ has been added as a dashed curve to Figure 3. It corresponds to $b = (2a-1)^{1/2}$. $\beta/\omega \ll 1$ corresponds therefore to $b \ll (2a-1)^{1/2}$ which should mean that b is close to unity or β is small, but positive. We note finally that the point corre-

sponding to the values ($a = 6.4$, $b = 4$) recommended by SALTZMAN *et al.* (1981) falls in the region $b > (2a-1)^{1/2}$.

BARAS *et al.* (1982) point out that simplifications of (3.13) may be made in the case where the radius $r(t)$ evolves to a nearly constant value, and that this is the case near a Hopf bifurcation point. Assuming therefore that $r(t)$ is almost constant we may average (3.13) with respect to ϕ using the operator

$$\tilde{(\ )} = \frac{1}{2\pi} \int_0^{2\pi} (\ )\, d\phi \tag{3.14}$$

We find under these rather severe assumptions that

$$0 \approx \frac{d\tilde{r}}{dt} = \beta\tilde{r} - \frac{1}{2}\tilde{r}^3$$

$$\tilde{\Omega} = \omega + \frac{3}{2}\frac{(1+\beta)}{\omega}\tilde{r}^2 \tag{3.15}$$

since all the other terms give no contributions to the means. $\tilde{\Omega}$ has been introduced to denote the mean angular velocity. (3.15) should thus be applicable to nearly circular limit cycles which occur close to the bifurcation point. The radius of the limit cycle is $r_0 = (2\beta)^{1/2}$. While the limit cycle is circular in the (r, ϕ) plane it will have another shape in the (η, ϕ) plane. Using (3.8) we may transform $r^2 = r_0^2$ back to the original co-ordinates, and we obtain

$$[(1+\beta)^2 + \omega^2]\,\eta^2 + \theta^2 - 2(1+\beta)\,\eta\theta = 8\beta\omega^2 \tag{3.16}$$

which also may be written in the form

$$a\eta^2 + \theta^2 - (b+1)\eta\theta = (b-1)\,(4a - (b+1)^2) \tag{3.17}$$

The approximate limit cycle is thus an ellipse in the (η, θ) co-ordinates.

The equation for the ellipse (3.17) can be written in the standard form by turning the (η, θ) co-ordinates an angle u, where

$$\tan 2u = -\frac{b+1}{a-1} \tag{3.18}$$

The equation is then

$$\frac{\eta_x^2}{A^2} + \frac{\theta_x^2}{B^2} = 1 \tag{3.19}$$

with

$$A^2 = \frac{2(b-1)(4a-(b+1)^2)}{a+1-\sqrt{R}}$$

$$B^2 = \frac{2(b-1)(4a-(b+1)^2)}{a+1+\sqrt{R}} \qquad R = (a-1)^2 + (b+1) \tag{3.20}$$

Figure 4 shows A, B and u as a function of b for $a = 6.4$. It is seen that u varies relatively little, that A is considerably larger than B and that B goes to zero when $b \to 2\sqrt{a} - 1$. At this limit it is noted that A^2 is of the type 0/0 but it is easy to see that the limiting value of A is $8(a - \sqrt{a})(a+1)/\sqrt{a}$. The main result is therefore that the approximate limit cycle is an ellipse which for increasing values of b and constant a attains larger and larger eccentricity and in the limit becomes a straight line.

Having investigated the approximate method of determining the limit cycle in some detail we may investigate the validity of this method. This has been done experimentally by integrating the system (3.1) until the limit cycle is reached. The numerical integrations were carried out using Heun's scheme. Figures 5A and 5B correspond to the case of $a = 6.4$, $b = 1.2$ or $\beta = 0.1$, $\omega = 2.28$. We notice excellent agreement between the two closed curves. The true limit cycle is slightly larger than the ellipse. There is also good agreement between the periods, 1652

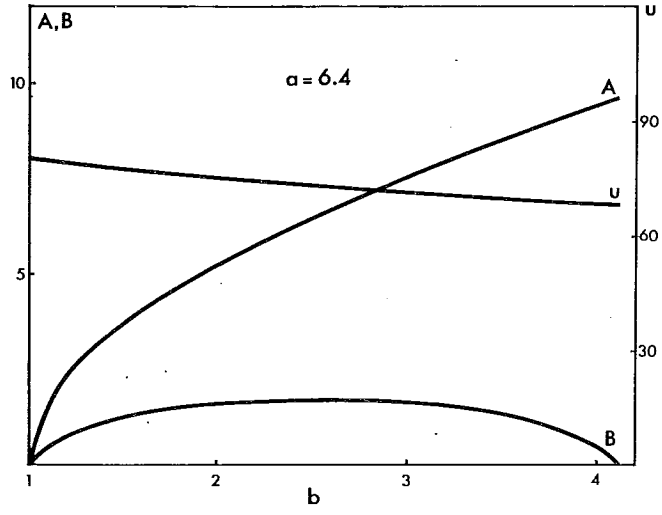

Figure 4. The half-axes A and B and the slope of the major axis of the ellipse as a function of b for a constant $a = 6.4$.

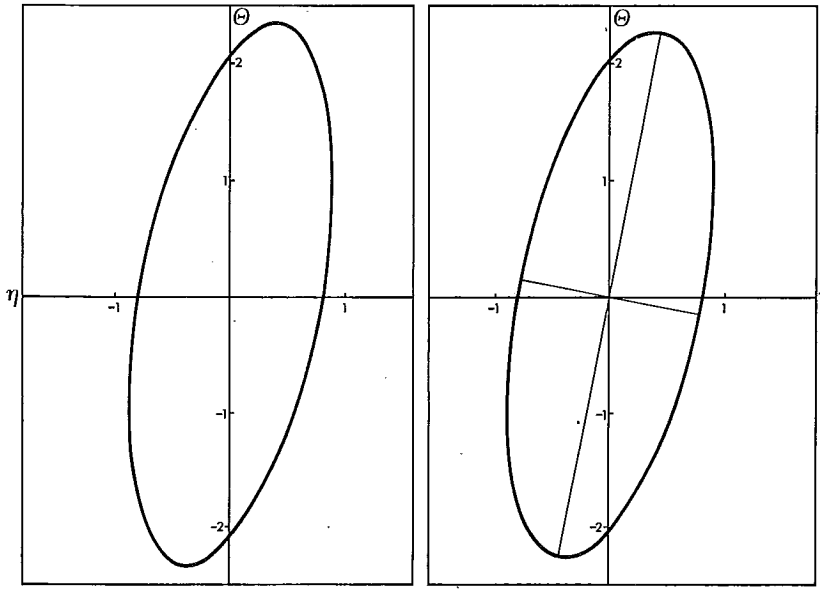

Figure 5A. Limit cycle obtained by numerical integration (a = 6.4, b = 1.2).
Figure 5B. Approximate limit cycle, a = 6.4, b = 1.2.

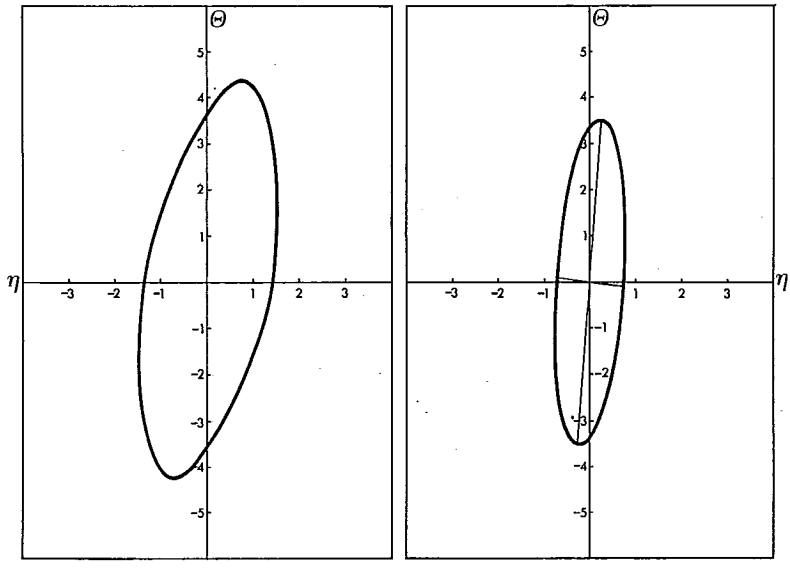

Figure 6A. As Figure 5A (a = 6.4, b = 1.6).
Figure 6B. As Figure 5B (a = 6.4, b = 1.6).

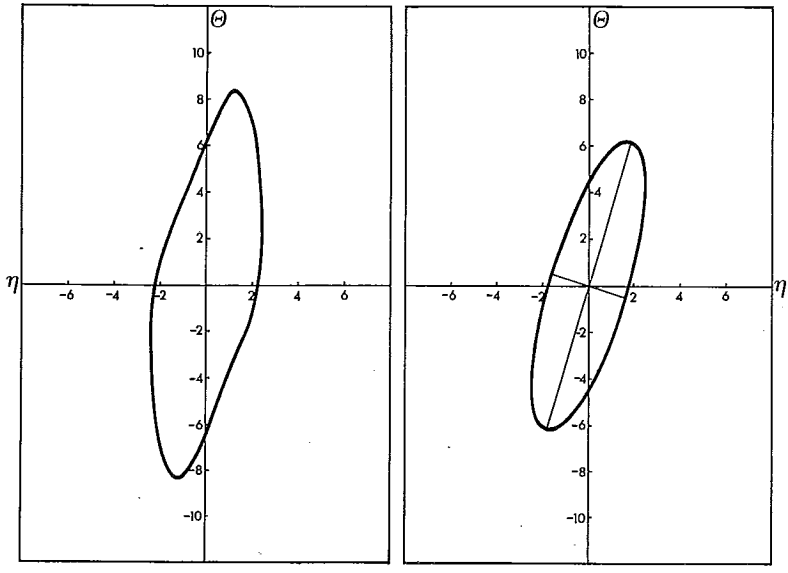

Figure 7A. As Figure 5A (a = 6.4, b = 2.5).
Figure 7B. As Figure 5B (a = 6.4, b = 2.5).

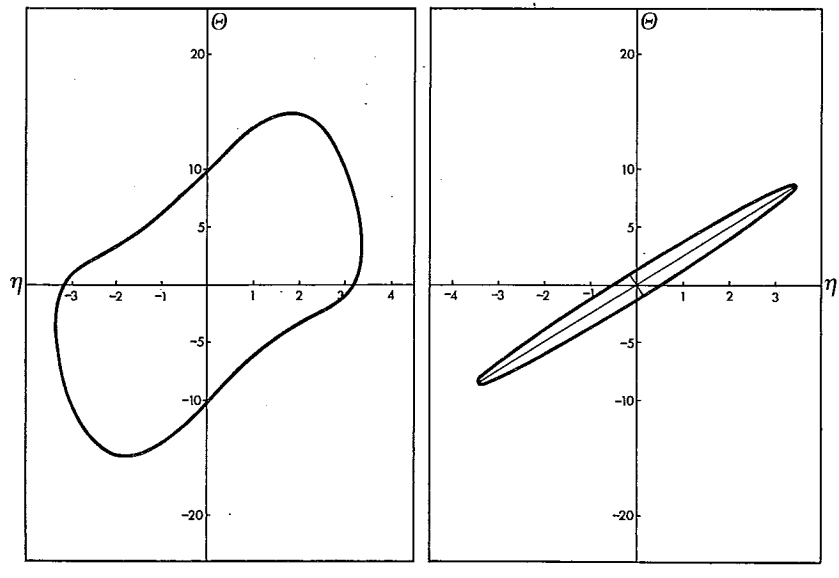

Figure 8A. As Figure 5A (a = 6.4, b = 4).
Figure 8B. As Figure 5B (a = 6.4, b = 4).

hours for the true limit cycle and 1645 hours for the ellipse. Figures 6A and 6B compare the cases $a = 6.4$, $b = 1.6$ or $\beta = 0.3$, $\omega = 2.17$. The differences between the two curves become even greater in Figures 7A, B and Figures 8A, B when β becomes larger. Large differences appear also in the periods. The period in the true limit cycle for Figure 7 is 1410 hours, while the period for the ellipse is 1001 hours. Figure 8 was calculated using the values of a and b recommended by SALTZMAN *et al.* (1981). As we have seen earlier the approximate method should not apply in this case because $\beta/\omega = 3.87$. Figure 8A and Figure 8B show clearly that the approximate method does not work at all in this case.

In conclusion we may state that the approximate method of determining the limit cycle is of value only very close to the bifurcation point. It does not apply in this case to the system of interest for the climate subsystem, because it is located very far from the bifurcation curve. It is as a matter of fact located very close to the curve where the limit cycle disappears.

4. *A system of two populations*

As the second example we shall select a biological system consisting of two populations, a so-called prey-predator system. Such models are studied in detail in the field of ecology. We shall not go into the ecological justification of the particular model treated here. It is only one of several models considered by MAY (1976). In the following $N(t)$ will denote the prey population and $P(t)$ the predator population. With t denoting time the equations are

$$\frac{dN}{d\tau} = rN\left(1 - \frac{N}{K}\right) - k\frac{PN}{N+D}$$

$$\frac{dP}{d\tau} = sP\left(1 - \gamma\frac{P}{N}\right) \tag{4.1}$$

where k, r, s, γ, K and D are constants. It is seen that r and s measure the intrinsic growth rates of the populations N and P, respectively, while K is the so-called carrying capacity for N. On the other hand, the corresponding quantity for P is N/γ, saying that the carrying capacity for P is proportional to N. The particular form of the last term in the first equation, measuring a decrease in N due to the interaction with P, is constructed in such a way that the predators are less effective at high prey densities when they as a matter of fact are most needed as a regulatory mechanism.

To ease the mathematical treatment we shall non-dimensionalize the equations as follows:

$$N = Dx, \quad P = \gamma^{-1} Dy, \quad \tau = r^{-1} t \tag{4.2}$$

resulting in the equations

$$\begin{aligned} \frac{dx}{dt} &= x\left(1 - \frac{x}{(K/D)}\right) - \frac{k}{r\gamma}\frac{xy}{1+x} \\ \frac{dy}{dt} &= \frac{1}{(r/s)}\, y\left(1 - \frac{y}{x}\right) \end{aligned} \tag{4.3}$$

In the following we shall use the notations $p = K/D$ as the non-dimensional carrying capacity and $q = r/s$ as the ratio of the growth rates. Following MAY (1976) we set $k/(\gamma r) = 1$. We may then write the equations in the form

$$\begin{aligned} (1+x)\frac{dx}{dt} &= x(1+x)\left(1 - \frac{x}{p}\right) - xy \\ x\frac{dy}{dt} &= \frac{1}{q}\, y(x-y) \end{aligned} \tag{4.4}$$

(4.4) has only one non-trivial steady state namely $x_s = y_s$ and x_s satisfying the equation

$$x_s(1 + x_s) = p \tag{4.5}$$

or

$$x_s = \left(p + \tfrac{1}{4}\right)^{\frac{1}{2}} - \tfrac{1}{2} \tag{4.6}$$

We denote the deviations from this steady state by x' and y', *i.e.*

$$\begin{aligned} x &= x_s + x' \\ y &= y_s + y' \end{aligned} \tag{4.7}$$

Substituting from (4.7) in (4.4) it is straightforward to write the equations for the rate of change of x' and x'. They are:

$$\begin{aligned} \frac{dx'}{dt} + \frac{1}{1+x_s}\, x'\frac{dx'}{dt} &= \frac{x_s^2 - x_s - 1}{(1+x_s)^2}\, x' - \frac{x_s}{1+x_s}\, y' \\ &\quad + \frac{x_s^2 - 2x_s - 1}{x_s(1+x_s)^2}\, x'^2 - \frac{1}{1+x_s}\, x'y' - \frac{1}{x_s(1+x_s)^2}\, x'^3 \\ \frac{dy'}{dt} + \frac{x'}{x_s}\frac{dy'}{dt} &= \frac{1}{q}\, x' - \frac{1}{q}\, y' + \frac{1}{qx_s}\, x'y' - \frac{1}{qx_s}\, y'^2 \end{aligned} \tag{4.8}$$

(4.8) is equivalent to (4.4). No additional approximations have been made. Considering only the linear terms we may perform the usual linear stability analysis and determine the eigenvalues. In this study we shall be interested only in the case when the eigenvalues are of the form $\beta \pm i\omega$ indicating instability when $\beta > 0$ and an oscillatory linear solution when $\omega \neq 0$. The results are that

$$2\beta = \frac{x_s^2 - x_s - 1}{(1+x_s)^2} - \frac{1}{q}\,; \quad 2\omega = \left[\frac{4}{q}\frac{1+2x_s}{(1+x_s)^2} - 4\beta^2\right]^{\frac{1}{2}} \tag{4.9}$$

The last relation in (4.9) may also be written in the form

$$\beta^2 + \omega^2 = \frac{1}{q}\frac{1+2x_s}{(1+x_s)^2} \tag{4.10}$$

Figure 9 shows the region in (p, q) space in which the linear solution is such that $\beta > 0$ (lower curve) and ω is real (upper curve). The region of interest is thus between the two curves. The eigenvectors are most easily found from the second equation in (4.8). The first transformation is

$$\begin{Bmatrix} x' \\ y' \end{Bmatrix} = \begin{Bmatrix} 1 + q(\beta + i\omega) & 1 + q(\beta - i\omega) \\ 1 & 1 \end{Bmatrix} \begin{Bmatrix} Z \\ Z_\star \end{Bmatrix} \tag{4.11}$$

and transforming into polar co-ordinates as in the previous section we obtain

$$\begin{aligned} x' &= 2(1+q\beta)\, r_c - 2q\omega r_s; \quad & r_c &= r\cos\phi \\ y' &= 2r_c\,; & r_s &= r\sin\phi \end{aligned} \tag{4.12}$$

From this point onwards we follow the same procedure as in the previous section ending eventually with equations for dr/dt and $d\phi/dt$. The intermediate algebra is long and cumbersome and is not reproduced here. The following equations are those which remain after the neglect of all those terms which have a fast variation in ϕ.

$$\begin{aligned} \frac{dr}{dt} &= \beta r - \frac{3}{2}\frac{1}{x_s(1+x_s)^2}\left[(1+q\beta)^2 + (q\omega)^2\right] r^3 \\ \frac{d\phi}{dt} &= \omega + \frac{3}{2}\frac{1+q\beta}{qx_s(1+x_s)^2}\left[(1+q\beta)^2 + (q\omega)^2\right] r^2 \end{aligned} \tag{4.13}$$

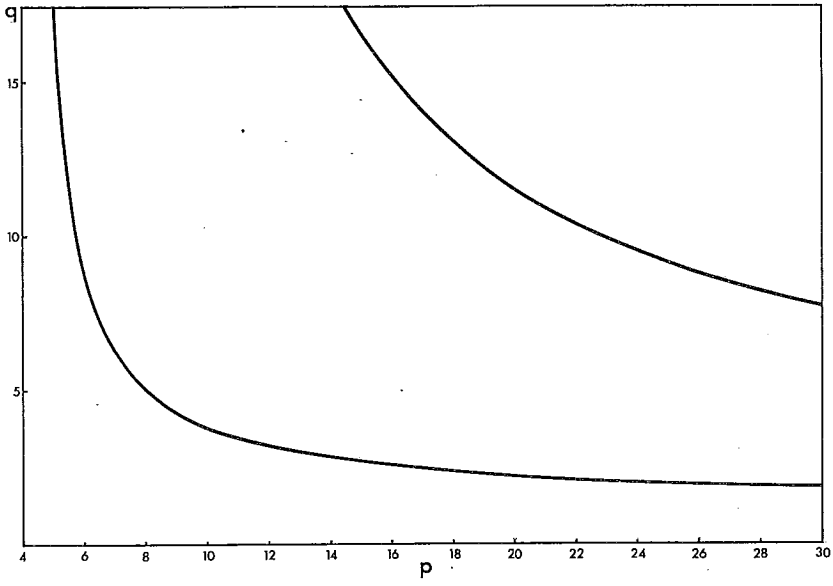

Figure 9. The region in which limit cycles may occur is between the two curves. The lower curve is $\beta = 0$.

The terms in the square brackets can be further reduced. Using (4.9) and (4.10) we get

$$(1 + q\beta)^2 + (q\omega)^2 = q \frac{x_s}{1 + x_s} \tag{4.14}$$

and the equations become

$$\begin{aligned} \frac{dr}{dt} &= \beta r - \frac{3}{2} \frac{q}{(1 + x_s)^3} r^3 \\ \frac{d\phi}{dt} &= \omega + \frac{3}{2} \frac{1 + q\beta}{\omega} \frac{1}{(1 + x_s)^3} r^2 \end{aligned} \tag{4.15}$$

The system (4.15) is naturally of the same form as (3.15) in the previous section because the same approximations have been made. We find therefore that according to these approximate equations we should have a circular limit cycle with a radius r_0 where

$$r_0^2 = \frac{2}{3} \frac{\beta(1 + x_s)^3}{q} \tag{4.16}$$

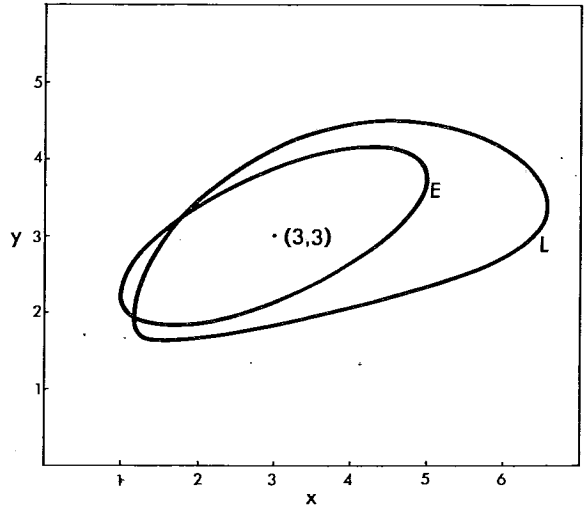

Figure 10. The closed curve marked L is the limit cycle obtained by numerical integration while the curve E is the approximate limit cycle ($p = 12$, $q = 4$).

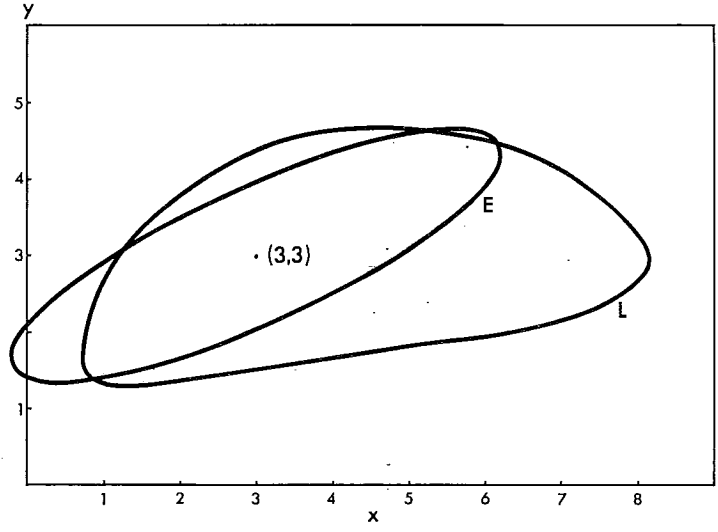

Figure 11. As Figure 10 ($p = 12$, $q = 5$).

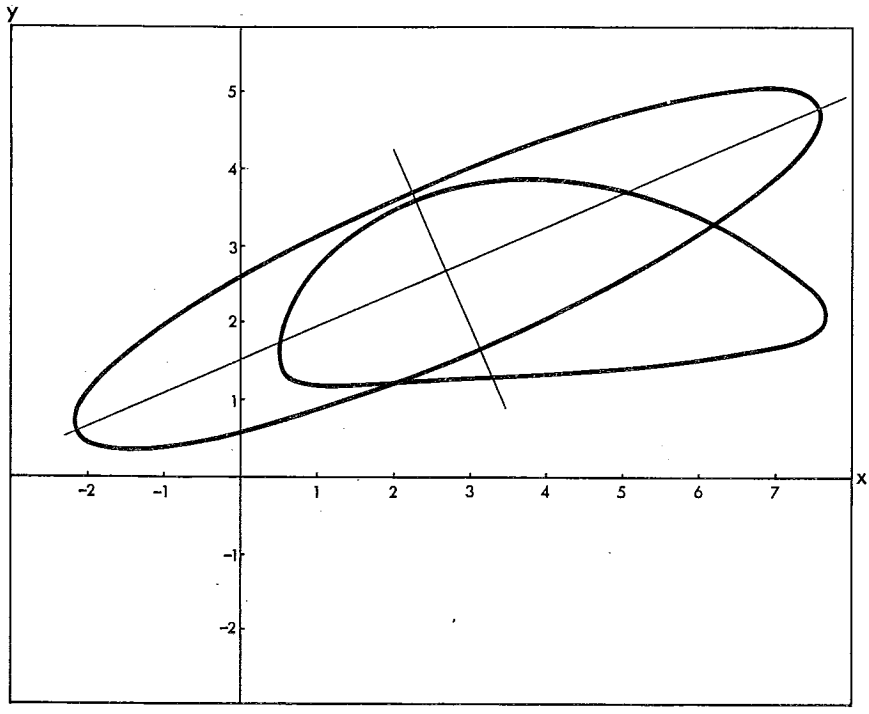

Figure 12. As Figure 10 (p = 10, q = 6).

Due to the transformations (4.12) it is also evident that the limit cycle will be an ellipse in (x', y') - space. The equation is:

$$x'^2 + q\frac{x_s}{1+x_s}y'^2 - 2(1+q\beta)x'y' = \frac{3}{8}\beta q\omega^2(1+x_s)^3 \tag{4.17}$$

We are therefore now in a position to compare the approximate elliptical limit cycle described by (4.17) with limit cycles determined by direct numerical integrations of the system (4.3). A few comparisons will be shown.

Figure 10 shows the numerically computed limit cycle, marked L, and the ellipse, marked E, for the case p = 12, q = 4. The steady state is (x_s, y_s) = (3,3). For this case we have β = 0.03 and ω = 0.33 showing that $\beta \ll \omega$. In spite of the smallness of β we do not find a close agreement between the two closed curves. The reason is probably that the limit cycle in the (r, ϕ) plane, even for small values of β and β/ω, is not a circle and therefore not an ellipse in the

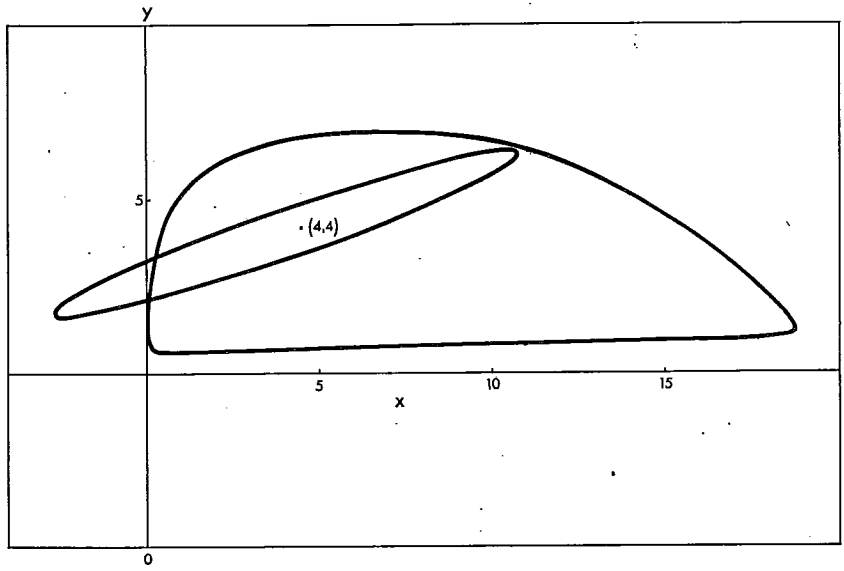

Figure 13. As Figure 10 (p = 20, q = 10).

(x', y') plane. This in turn is related to the structure of the basic equations (4.4) in which additional non-linearities appear on the left hand sides, *i.e.* the terms $x'(dx'/dt)$ and $x'(dy'/dt)$. We see in Figure 10 that L is asymmetric around the steady state (3, 3) while E by definition is symmetric. Consequently, a very close agreement is impossible.

The same discrepancy is seen in Figure 11, calculated with p = 12, q = 5 leading to (x_s, y_s) = (3, 3) and β = 0.056, ω = 0.27. The approximate limit cycle (E) is even reaching into the region $x < 0$ in this case. An even more extreme example is shown in Figure 12 with p = 10, q = 6 leading to (x_s, y_s) = (2.7, 2.7) and β = 0.048, ω = 0.275. Finally, in Figure 13 we show an example when p = 20, q = 10, $x_s = y_s$ = 4, β = 0.17, ω = 0.084, *i.e.* a case in which $\beta/\omega > 1$. As in the previous case the ellipse has now become quite extreme with $B/A \ll 1$ while the true limit cycle bears no resemblance to the ellipse.

5. *Conclusions*

The investigation described in this paper explores the extent to which a certain approximate method for the determination of a limit cycle can be used. The method can be justified for certain types of nonlinear, coupled, ordinary differ-

ential equations operating close to a Hopf bifurcation. The requirement is that the amplification rate β should be small compared to the frequency ω of the oscillatory motion.

The system considered in section 3 is a simple model of the interaction between the ocean temperature and the extent of the polar sea ice. The form of the governing equations is such that it can be expected that approximate method should work if the conditions for its validity are satisfied, *i.e.* $\beta/\omega \ll 1$. The accuracy of the approximate method is investigated by comparing »true» limit cycles obtained by numerical integrations of the giverning equations with the ellipses which are the approximate limit cycles. The results are that excellent agreement is found for $\beta = 0.1$, $\omega = 2.28$, but $\beta = 0.3$, $\omega = 2.17$ already shows a considerable difference between the two closed curves especially with respect to the amplitude of the oscillation in temperature. These differences increase as β becomes larger, and when β and ω attain the values which supposedly are relevant to the natural system, *i.e.* $\beta = 1.5$, $\omega = 0.39$, the approximate method has broken down completely with respect to accuracy in all parameters.

We may thus conclude that the approximate method unfortunately does not apply to the climate sub-system under investigation. The main reason is that the natural system operates far from the Hopf bifurcation.

The second example treated in Section 4 is taken from theoretical ecology. It describes the interaction between two competing populations. Although the form of the equations in this case is not of the required form one may still hope that the approximate method will work close to the bifurcation point. A reasonable, but far from excellent agreement exists indeed for $\beta/\omega \ll 1$, but it is also seen that the true limit cycle even for these values deviates systematically from the elliptic form. Comparisons made for larger values of β/ω bring this difference out more clearly, and once again the approximate method breaks down completely far from the bifurcation point.

It is naturally desirable to have methods by which it is possible to determine limit cycles by analytical methods even if such methods involve approximations. If such methods apply to a natural system they may be used for a much more detailed theoretical treatment of the system. The method investigated in this paper appears to work with sufficient accuracy only quite close to the bifurcation point and cannot be applied with confidence to systems which operate far from this point as has been attempted by other investigators.

REFERENCES

BARAS, F., M. MALEK-MANSOUR and C. van DEN BROECK, 1982: Asymptotic properties of coupled nonlinear Langevin equations in the limit of weak noise. II: Transition to a limit cycle, *Jour. Stat. Phys.*, **28**, 577–587.

KÄLLÉN, E., C. CRAFOORD and M. GHIL, 1979: Free oscillations in a climate model with ice-sheet dynamics, *Jour. Atmos. Sci.* **36**, 2292–2303.

– » – and A. WIIN-NIELSEN, 1980: Nonlinear, low order interactions, *Tellus*, **32**, 393–409.

MAY, R., 1976: *Theoretical Ecology.*

SALTZMAN, B., 1982: Stochastically-driven climatic fluctuations in the sea-ice, ocean temperature, CO_2 feedback system, *Tellus*, **34**, 97–112.

–»– and R.E. MORITZ, 1980: A time-dependent climatic feedback system involving sea-ice extent, ocean temperature and CO_2, *Ibid.*, **32**, 93–118.

–»– , A. SUTERA and A. EVENSON, 1981: Structural stochastic stability of a simple auto-oscillatory climate feedback system, *Jour. Atmos. Sci.*, **38**, 494–503.